



Toffoli, A., Bitner-Gregersen, E., Onorato, M., Babanin, A. V. (2008). Wave-induced upper-ocean mixing in a climate model of intermediate complexity

Originally published in *Ocean Engineering*, 35 (17-18), 1784-1792

Available from:

<http://dx.doi.org/10.1016/j.ocemod.2009.04.003>

Copyright © 2008 Elsevier Ltd. All rights reserved.

This is the author's version of the work. It is posted here with the permission of the publisher for your personal use. No further distribution is permitted. If your library has a subscription to this journal, you may also be able to access the published version via the library catalogue.



Wave crest and trough distributions in a broad-banded directional wave field

A.Toffoli, E.Bitner-Gregersen, M.Onorato, A.V.Babanin

Abstract

It is well established that the modulational instability enhances the probability of occurrence for extreme events in long crested wave fields. Recent studies, however, have shown that the coexistence of directional wave components can reduce the effects related to the modulational instability. Here, numerical simulations of the Euler equations are used to investigate whether the modulational instability may produce significant deviations from second-order statistical properties of surface gravity waves when short crestness (i.e., directionality) is accounted for. The case of a broad-banded directional wave field (i.e. wind sea) is investigated. The analysis is concentrated on the wave crest and trough distribution. For completeness a comparison with a unidirectional wave field is presented also. Results will show that the distributions based on second-order theory provide a good estimate for the simulated crest and trough height also at low probability levels.

Keywords: Directional wave field, Euler equations, Nonlinear waves, Wave crest distribution, Wave trough distribution.

1. Introduction

The statistical description of the wave amplitude represents a fundamental input for many practical applications. For the design of marine structures, for example, the probability distribution of the crest elevation (i.e., the highest elevation of an individual wave) must be established with care as it is used for the calculation of wave loads. Furthermore, a proper statistical knowledge of extreme crests is essential to define a sufficient air gap under the platform deck, and hence to ensure that a wave crest does not endanger the structure's integrity. Although the analysis of the wave crest distribution has received more attention, also the statistical description of wave troughs (i.e., the deepest depression of individual waves) is of importance for a number of engineering applications. For example, it is essential to define the maximal trough depth in the design of offshore rigs, because underwater cross-bars must not be exposed to the air, but at the same time should be sufficiently close to the surface. The wave trough distribution, moreover, is of importance also for specification of tether loads when designing tension-leg platforms.

Today it is common practice to describe the surface elevation by taking into account bound modes up to the second order, i.e. second-order wave theory (Hasselmann, 1962; Longuet-Higgins,

1963), from which probabilistic models for the crests and troughs can be developed (see, for example, Tayfun, 1980; Arhan and Plaisted, 1981; Forristall, 2000; Prevosto et al., 2000; Tayfun and Fedele, 2007b). Among them, the wave crest distributions proposed by Forristall (2000) are frequently used for engineering calculations. However, although exploration of this approach has already proved a relatively good agreement with observations, there are measurements that clearly show significant discrepancies especially at low probability levels (Bitner-Gregersen and Magnusson, 2004; Petrova et al., 2006).

In this respect, when waves are long crested, i.e. unidirectional, narrow banded and in water of infinite depth, the modulational instability of free wave packets can develop (Onorato et al., 2001, 2006; Janssen, 2003). As a result, the statistical properties of surface gravity waves can significantly diverge from the ones calculated by second-order theory (see, e.g., Mori and Yasuda, 2002; Onorato et al., 2006; Gibson et al., 2007). Using direct numerical simulations of the Euler equations, furthermore, Toffoli et al. (2008) have demonstrated that the effects related to free wave modes can enhance the crest height up to 20%, at probability levels as low as 0.001. However, for the more realistic case of short crested waves (local wind sea), where wave components with different directions of propagation coexist, the effect of the modulational instability is reduced (Onorato et al., 2002a; Socquet-Juglard et al., 2005; Waseda, 2006; Gramstad and Trulsen, 2007). Socquet-Juglard et al. (2005), in particular, using higher order nonlinear Schrödinger-type equations (Dysthe, 1979), have shown that the modulational instability does not yield any significant deviation of the wave crest distribution from the

theoretical second-order based distribution proposed by Tayfun (1980) in broad directional wave fields. However, the Schrödinger-type equations are limited to narrow-banded spectra (both in frequency and direction). It is therefore not yet clear whether the modulational instability may significantly change the statistical properties of surface gravity waves when more broad-banded spectral conditions are considered.

The present study attempts to address this problem by using numerical simulations of the Euler equations to describe the statistical properties of a broad-banded, short crested wave field in water of infinite depth. For comparison, simulations of long crested wave fields have also been performed. Although some approximations are needed to carry out the simulations, the Euler equations account for both the effects related to bound modes of second and higher order and the ones related to free modes. Moreover, this approach does not have any bandwidth constraints unlike the nonlinear Schrödinger-type equations used in Socquet-Juglard et al. (2005).

A brief description of the model and the initial conditions taken into account are presented in the next section. In Section 3, the statistical properties of the simulated directional wave fields are compared with results for unidirectional waves. Although directional effects have not been investigated comprehensively (only one type of directional distribution has been taken into account), we show that directionality has a significant effect on the formation of extreme waves, substantially reducing their probability of occurrence. In Section 4, the shape of the simulated wave crest distributions is investigated and compared with distributions based on second-order wave theory; the effect of the selected directional spreading on the tail of the distribution is discussed. A similar analysis is then extended to the probability distribution of the wave troughs (Section 5). Concluding remarks are presented in the last section.

2. The numerical experiment

2.1. The model

In the case of constant water depth ($h = \infty$ in this study), the velocity potential $\phi(x, z, t)$ of an irrotational, inviscid, and incompressible liquid satisfies the Laplace's equation everywhere in the fluid. The boundary conditions are such that the vertical velocity at the bottom ($z = -\infty$) is zero, and the kinematic and dynamic boundary conditions are satisfied for the velocity potential $\psi(x, y, t) = \phi(x, y, \eta(x, t), t)$ on the free surface, i.e., $z = \eta(x, y, t)$ (see Zakharov, 1968). The expressions of the kinematic and dynamic boundary conditions are as follows:

$$\psi_t + g\eta + \frac{1}{2}(\psi_x^2 + \psi_y^2) - \frac{1}{2}W^2(1 + \eta_x^2 + \eta_y^2) = 0, \quad (1)$$

$$\eta_t + \psi_x \eta_x + \psi_y \eta_y - W(1 + \eta_x^2 + \eta_y^2) = 0, \quad (2)$$

where the subscripts denote the partial derivatives, and $W(x, y, t) = \phi_{z|\eta}$ represents the vertical velocity evaluated at the free surface.

The time evolution of the surface elevation can be calculated from Eqs. (1) and (2). Numerical simulations of these equations, however, are rather complex. For this study, we have used the higher order spectral method (HOSM), which was independently proposed by West et al. (1987) and Dommermuth and Yue (1987). A comparison of these two approaches (Clamond et al., 2006) has shown that the formulation proposed by Dommermuth and Yue (1987) is less accurate than the one proposed by West et al. (1987). The latter, therefore, has been applied for the present study.

HOSM uses a series expansion in the wave slope of the vertical velocity $W(x, y, t)$ about the free surface. Herein we have considered a third-order expansion so that the four-wave interaction is included (see Tanaka, 2001b, 2007); note, however, that the solution is not fully nonlinear. The expansion is then used to evaluate the velocity potential $\psi(x, y, t)$ and the surface elevation $\eta(x, y, t)$ from Eqs. (1) and (2) at each instant of time. All aliasing errors generated in the nonlinear terms are removed (see West et al., 1987; Tanaka, 2001b for details). The time integration is performed by means of a four-order Runge–Kutta method. A concise review of HOSM can be found in Tanaka (2001a).

Note that other numerical approaches can be found in the literature (see, for example Tsai and Yue, 1996, for a review). Promising methods have also been proposed by Annenkov and Shrira (2001), Clamond and Grue (2001), and Zakharov et al. (2002). A comparative analysis between the performance of the HOSM and other numerical approaches can be found in Clamond et al. (2006).

2.2. Initial conditions and simulations

For the construction of the initial conditions, a directional wave spectrum $E(\omega, \theta) = S(\omega)D(\omega, \theta)$ is used, where $S(\omega)$ represents the frequency spectrum and $D(\omega, \theta)$ is the directional function. As it is frequently used for many practical applications, the JONSWAP formulation (see, e.g., Komen et al., 1994) is herein adopted to describe the energy distribution in the frequency domain. In the present study, for convenience, we have chosen a peak period $T_p = 4$ s, which corresponds to a dominant wavelength $\lambda_p = 25$ m, and Phillips parameter $\alpha = 0.014$. Note that the choice of the peak period is arbitrary, and any other wave period representing wind sea could have been applied. Different values for the peak enhancement factor γ , then, have been selected to describe different significant wave heights (H_s). This choice is twofold: (i) it defines different degrees of nonlinearity as measured by the wave steepness $k_p a$ (the higher the steepness, the more important the contribution of nonlinear terms), where k_p is the wavenumber related to the dominant wavelength and a is half the significant wave height; (ii) it defines different values of the Benjamin–Feir Index (BFI), which measures the relative importance of nonlinearity and dispersion (see Onorato et al., 2001; Janssen, 2003). The BFI is here calculated as the ratio of the wave steepness $k_p a$ to the spectral bandwidth $\Delta k/k_p$, where Δk is a measure of the width of the spectrum estimated as the half-width at the half-maximum (see for details Onorato et al., 2006). Note that, for narrow-banded wave trains, the non-resonant interaction between free modes gives rise to a much larger deviation from the Gaussian statistics than bound waves if $\text{BFI} = O(1)$ (Janssen, 2003; Mori and Janssen, 2006). The values of the peak enhancement factor γ , wave steepness and BFI are summarized in Table 1. These values are related to the selected JONSWAP spectra only, and hence do not contain any information regarding directionality. We also mention that the concurrent values of the steepness are representative for rather extreme sea states (see, e.g., Toffoli et al., 2005; Socquet-Juglard et al., 2005), which are of interest for practical applications.

Table 1
Parameters of numerical experiments

γ	H_s	$k_p a$	BFI
1.0	0.84	0.106	0.20
3.3	1.04	0.131	0.70
6.0	1.20	0.151	1.00

A $\cos^{2s}(\theta/2)$ function is then applied to model the energy in the directional domain. Several definitions for the spreading coefficient s can be found in the literature (see, e.g., [Ewans, 1998](#) for a concise review). For the present study, we have chosen the formulation proposed by [Mitsuyasu et al. \(1975\)](#) so that at the peak frequency $s(\omega_p) = 10$. Considering that the mean direction of propagation is equal to zero, the selected function and directional spreading distribute the energy on a range of $\pm 25^\circ$.

From the directional-frequency spectrum, $E(\omega, \theta)$, an initial two-dimensional surface $\eta(x, y, t = 0)$ is computed using first the linear dispersion relation to move from (ω, θ) to wavenumber coordinates (k_x, k_y) , and then the inverse Fourier transform with the random phase approximation. In this respect, the random phase ε is assumed to be uniformly distributed over the interval $[0, 2\pi]$. Note that also random amplitudes should be used to include the natural variability of waves. For the present simulations, therefore, we have assumed that the amplitudes are Rayleigh distributed (see, e.g., [Prevosto, 1998](#)). The velocity potential $\psi(x, y, t = 0)$ is obtained from the input surface using linear theory (see, e.g., [Whitham, 1974](#)). The wave field is contained in a square domain of 225 m with spatial mesh of 256×256 nodes. The selected resolution of the physical domain allows that the maximum mode number, k_{max} , corresponds to the sixth harmonic of the peak of the spectrum after the mode numbers k affected by aliasing errors are removed. It is important to mention that, in the present study, we are interested in the effect of the modulational instability mechanism, i.e., a quasiresonant four-wave interaction process that takes place near the peak of the spectrum. Therefore, the removal of aliasing errors should not have any influence on the results.

For comparison, unidirectional wave trains $\eta(x, t)$ have also been simulated using the Euler equations. To this end, we have used the same input frequency spectra $S(\omega)$ which have been selected for the simulations of the directional wave fields. Theoretical and numerical studies ([Janssen, 2003](#); [Socquet-Juglard et al., 2005](#)) have shown that deviations from the Gaussian statistics due to the modulational instability mechanism occur on a short timescale, typically on the order of 10 wave periods. In the present study, therefore, the total duration of the simulation is set equal to $100T_p$ so that the effects of modulational instability are captured. A small time step, $\Delta t = T_p/100 = 0.04$ s, is used to minimize the energy leakage; note that the selected time step is much smaller than the period of the shortest waves considered in this study. The accuracy of the computation is checked by monitoring the variation of the total energy E_{tot} (see, e.g., [Tanaka, 2001a](#)). An example of the variation of the total energy is shown in [Fig. 1](#) for the case $BFI = 1.0$. Despite the fact that the energy

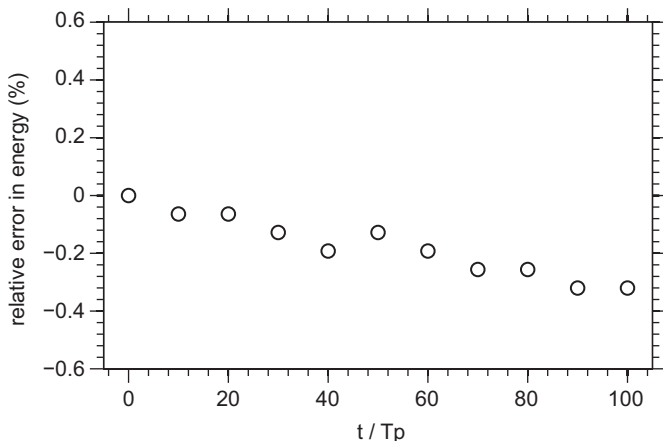


Fig. 1. Temporal variability of the total energy E_{tot} .

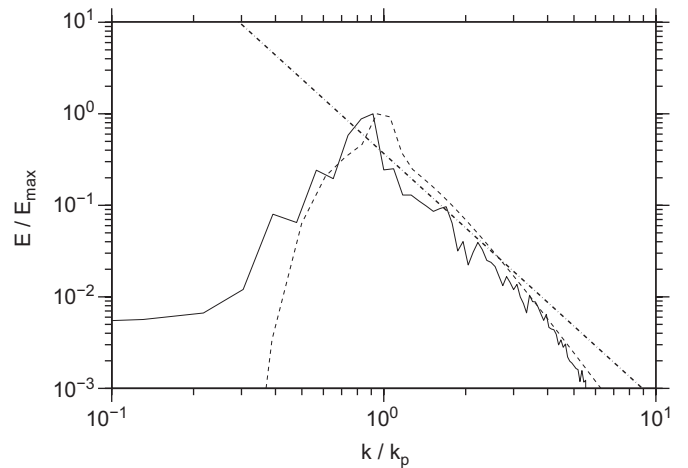


Fig. 2. Evolution of the energy spectrum: $t = 0T_p$ (dashed line); $t = 100T_p$ (solid line); power law $k^{-5/2}$ (dash-dotted line).

content shows a decreasing trend throughout the simulation, its variation is negligible as the relative error in E_{tot} does not exceed -0.4% (this result is consistent with similar simulations performed by [Tanaka, 2001a](#)).

For each instant of time, the skewness (λ_3) and kurtosis (λ_4) of the surface elevation are stored. It is not clear, however, how to extract individual waves from the two-dimensional surface $\eta(x, y, t)$. For the investigation of the crest and trough distributions, therefore, a time series analysis (down-crossing waves) of the surface elevation has been performed. To this end, time series have been collected from five different grid points to ensure enough samples for the statistical analysis, starting at time $t = 40T_p$. This choice has been motivated by the fact that after a time of $30-40T_p$, the statistical properties of the surface elevations reaches a statistically stable condition. Furthermore, the grid points have been chosen to ensure that the collected time series are independent realizations, i.e., the cross-correlation of the time series collected at two arbitrary grid points can be regarded as negligible.

Many repetitions (≈ 100) have been performed with different initial surfaces (i.e., different random amplitudes and phases). Approximately 30 000 individual waves have been considered.

It is important to mention that the spectral shape changes as the wave field evolves in time. Therefore, the wave spectrum at the last time step differs from the input spectrum. As an example, we show the normalized, integrated wavenumber spectrum at the initial condition and after 100 peak periods in [Fig. 2](#). As the wave field evolves, part of the energy is transferred towards low wavenumbers, yielding the downshift of the spectral peak. Furthermore, there is a clear tendency towards a $k^{-5/2}$ power law in the high wavenumber spectral tail. More detailed analysis of the spectral evolution can be found in [Tanaka \(2001b\)](#), [Onorato et al. \(2002b\)](#), [Socquet-Juglard et al. \(2005\)](#).

3. Skewness and kurtosis

In the following section, we discuss the effect of short crestness on the skewness and kurtosis of the surface elevation. Whereas the first describes the degree of vertical asymmetry, the latter refers to the occurrence of large events. For a Gaussian, linear, random process, the following values should be expected: $\lambda_3 = 0$; $\lambda_4 = 3$. In [Figs. 4 and 5](#), the skewness and kurtosis of the simulated time series are presented as a function of the BFI; both the unidirectional and directional case are shown. It is important

to mention that a large number of time series are needed to calculate stable statistical moments (see Bitner-Gregersen and Hagen, 2003). In this respect, we have verified that the collected time series are long enough to satisfy their stability (see, for example, Fig. 3).

It is well known that the vertical asymmetry of the wave profile becomes more pronounced if the wave steepness, and hence the BFI, increases; wave crests tend to be sharper and higher, while wave troughs become shallower and flatter. Consequently, the skewness departs from the values expected for Gaussian processes (see Fig. 4). As shown in Toffoli et al. (2008), only bound modes significantly contribute to this deviation (cf. Janssen, 2003; Mori and Janssen, 2006). When directional sea states are simulated, however, the skewness decreases, because coexisting directional components limit the nonlinear effects of bound modes (see, e.g., Forristall, 2000; Toffoli et al., 2006). For all cases examined herein, the skewness of the directional field shows an approximately constant reduction of about 28% if compared with the concurrent unidirectional simulations.

For long crested, deep water waves, on the other hand, the kurtosis is dominated by the nonlinear interaction between free modes. Apart from the experiment with BFI = 0.2, the kurtosis reaches significantly high values, $\lambda_4 > 3.45$, if compared with the

contribution of bound modes, which leads on average to $\lambda_{4(\text{bound})} = 3 + 24 (k_p H_s / 4)^2 \approx 3.12$ (see, for example, Mori and Janssen, 2006, for details). However, when a broad-banded directional distribution is considered, the contribution of free modes is substantially reduced. Although a certain dependency from the degree of nonlinearity (BFI) is still visible (see Fig. 5), the simulations show that the kurtosis does not significantly diverges from the values expected for linear and second-order waves. This result is consistent with numerical simulations of directional sea states that were performed with higher order nonlinear Schrödinger-type equations by Onorato et al. (2002a), and laboratory experiments conducted in a directional wave basin (Waseda, 2006).

For completeness, it is instructive to look at the temporal evolution of the kurtosis, which is presented in Fig. 6 for the case BFI = 1.0; note that here the kurtosis represents an ensemble average value for the surface elevation at each considered time step. When the wave field is unidirectional, the modulational instability occurs on a short time scale and a strong departure from Gaussian statistics is observed at about 40 peak periods. If directional components are accounted for, on the other hand, the kurtosis does not show any substantial departure from the values expected in linear and second-order theory. A few runs performed for longer temporal evolution (up to $500T_p$),

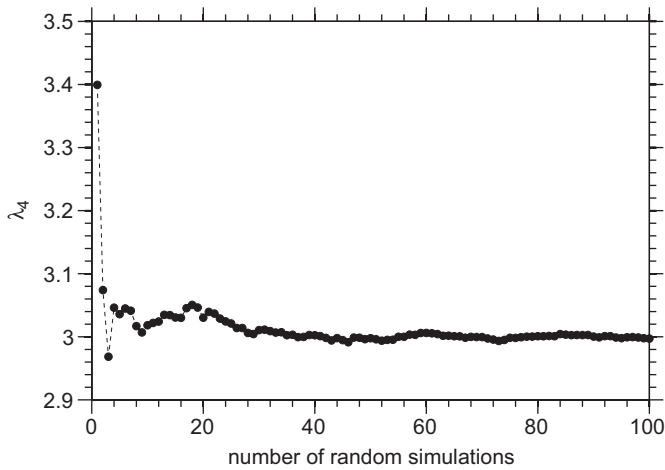


Fig. 3. Kurtosis as a function of the number of random simulations.

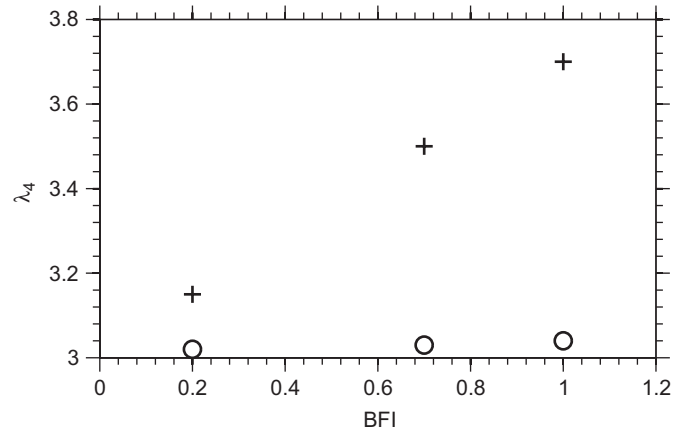


Fig. 5. Kurtosis (λ_4) as a function of the Benjamin-Feir Index (BFI): long crested waves (+); short crested waves (o).

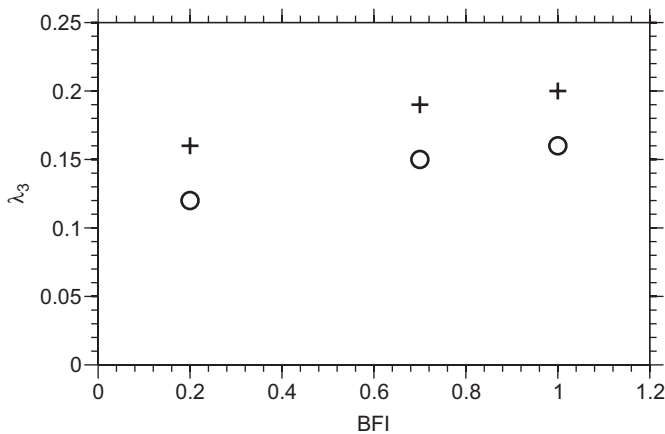


Fig. 4. Skewness (λ_3) as a function of the Benjamin-Feir Index (BFI): long crested waves (+); short crested waves (o).

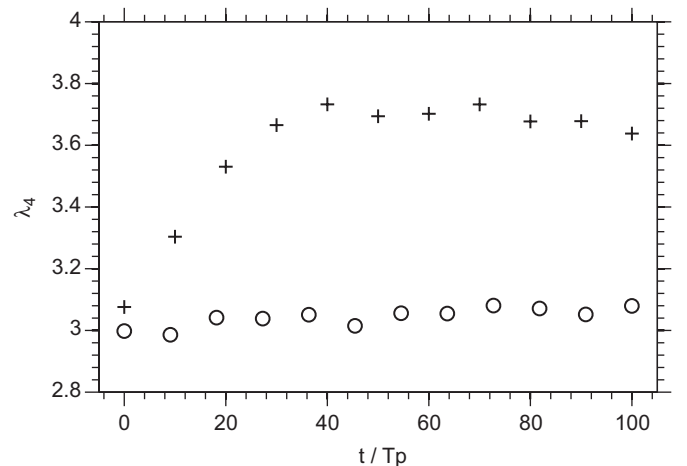


Fig. 6. Temporal evolution of the kurtosis (BFI = 1.0): unidirectional wave field (+); directional wave field (o).

moreover, have shown that the absence of substantial deviation from Gaussian statistics is a robust feature of broad directional wave fields. It can therefore be concluded that simulations of the Euler equations indicate that extreme wave events in a broad-banded, short crested wave field seem to be neither more frequent nor higher than the second-order theory predicts.

4. The wave crest distribution

In the following, a numerical distribution of wave crests generated from the Euler equations is compared with the predictions given by the second-order Tayfun (1980) and Forristall (2000) distributions.

The distribution proposed by Tayfun (1980) is derived by assuming that second-order, deep water waves with a narrow-banded spectrum can be described in a simplified form in which each realization of the surface elevation becomes an amplitude-modulated Stokes wave with a mean frequency and a random phase. Further, it does not include explicitly directional spreading.

In the case of a narrow-banded spectrum, the second-order surface elevation in the infinite water depth can be expressed as an envelope with a slowly varying amplitude and phase (see Tayfun, 1980):

$$\eta(x, t) = a_r(x, t) \cos(\theta) + \frac{1}{2} k_p a_r^2(x, t) \cos(2\theta), \quad (3)$$

where $\theta = k_p x - \omega t + \varepsilon$ and $a_r(x, t)$ is the slowly varying envelope. The second term on the right-hand side of Eq. (3) generates the Stokes-type contribution, which is a high frequency signal with a local maximum for each crest and trough. It is therefore straightforward to show that the wave crest assumes the following expression:

$$\eta_c = a_r + \frac{1}{2} k_p a_r^2. \quad (4)$$

Under the hypothesis that the linear wave amplitude is Rayleigh distributed, Eq. (4) can be used to derive an expression for the exceedance probability of the crest height (see Tayfun, 1980 for details); the latter can be written as follows:

$$P(\eta_c > \eta) = \exp \left[-\frac{8}{H_s^2 k_p^2} \left(\sqrt{1 + 2k_p \eta} - 1 \right)^2 \right]. \quad (5)$$

Note that the wave crest distribution in Eq. (5), known as the Tayfun distribution, represents a general expression, describing both long and short crested wave fields (Fedele and Arena, 2005; Tayfun, 2006; Tayfun and Fedele, 2006a, b, 2007b), when a fixed location is considered, i.e. an envelope in time. Nonetheless, by simulating long and short crested, second-order wave profiles, Forristall (2000) has shown that the directional spreading actually reduces the effect of second-order interaction, and hence modifies the tail of the wave crest distribution (see also Toffoli et al., 2006). For deep water waves, in this respect, the simulations of directional wave fields indicate that the crest height is slightly lower than the one obtained from the simulations of unidirectional wave trains, confirming findings reported earlier in the literature by several authors.

Furthermore, based on a large amount of second-order numerical simulations for the JONSWAP spectrum, Forristall (2000) has proposed a two-parameter Weibull fit for both unidirectional and directional waves. For the latter case, the directional distribution was described by a $\cos^{2s}(\theta/2)$ function with the spreading coefficient defined as in the work by Ewans (1998). The parameters of the Weibull distributions have been defined as functions of the average wave steepness and Ursell number. For short crested wave fields the two-parameter Weibull

crest distribution is as follows:

$$P(\eta_c > \eta) = \exp \left[-\left(\frac{\eta}{\alpha_w H_s} \right)^{\beta_w} \right], \quad (6)$$

where

$$\alpha_w = 0.3536 + 0.2568S_1 + 0.0800Ur, \quad (7)$$

$$\beta_w = 2 - 1.7912S_1 - 0.5302Ur + 0.2840Ur^2. \quad (8)$$

S_1 and Ur are the mean steepness and the Ursell number respectively:

$$S_1 = \frac{2\pi H_s}{g T_{01}^2}, \quad (9)$$

$$Ur = \frac{H_s}{k_{01}^2 h^3}, \quad (10)$$

where T_{01} is the mean wave period calculated from the ratio of the first two moments of the wave spectrum, k_{01} is the associated wavenumber, and h is the water depth. It is straightforward to note that the term in Eq. (10) is zero for deep water waves ($k_{01}h \rightarrow \infty$). The wave crest distribution in Eq. (6) will be referred to as the Forristall distribution hereafter.

Note that the directional distribution chosen by Forristall (2000) is slightly narrower than the one used for the present study. Recently, however, Toffoli et al. (2006) have shown that the statistical properties of second-order, directional wave fields are not significantly influenced by the value assumed by the directional spreading coefficient. It is important to mention, nonetheless, that the Weibull fit method proposed by Forristall (2000) is strictly applicable for unimodal spectra only. Second-order simulations performed by Bitner-Gregersen and Hagen (2003), however, showed that the crest height in bimodal spectra were somewhat higher than those in unimodal spectra conditions and were under predicted by the Forristall distribution.

In Figs. 7–9, the second-order wave crest distributions of Tayfun and Forristall (Eqs. (5) and (6)) are compared with the numerical simulations of the Euler equations (Eqs. (1) and (2)) for both long and short crested wave fields. As aforementioned, for long crested and narrow-banded wave trains, the dynamics of free modes increases the probability of occurrence of extreme waves. In the case of a small value of the BFI (0.2 in this study), the modulation instability does not have a significant effect on the

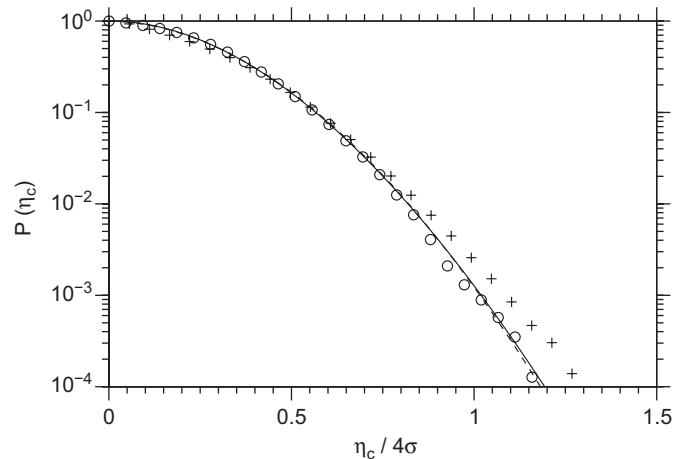


Fig. 7. Wave crest distribution for BFI = 0.2: Tayfun distribution (solid line); three-dimensional Forristall distribution (dashed line); simulations of long crested waves from the Euler equations (+); simulations of short crested waves from the Euler equations (o).

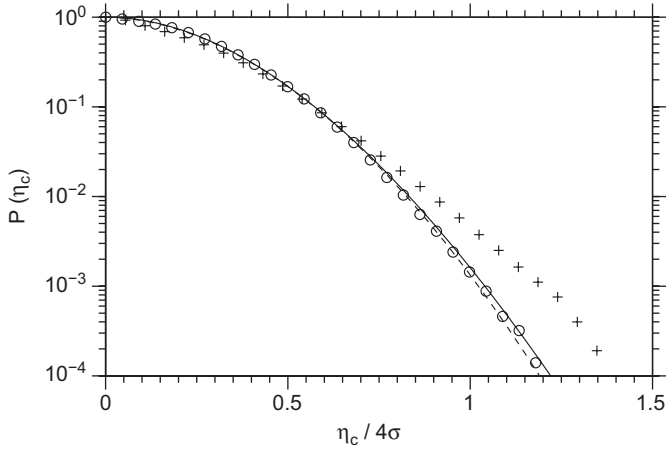


Fig. 8. Wave crest distribution for BFI = 0.7: Tayfun distribution (solid line); three-dimensional Forristall distribution (dashed line); simulations of long crested waves from the Euler equations (+); simulations of short crested waves from the Euler equations (o).

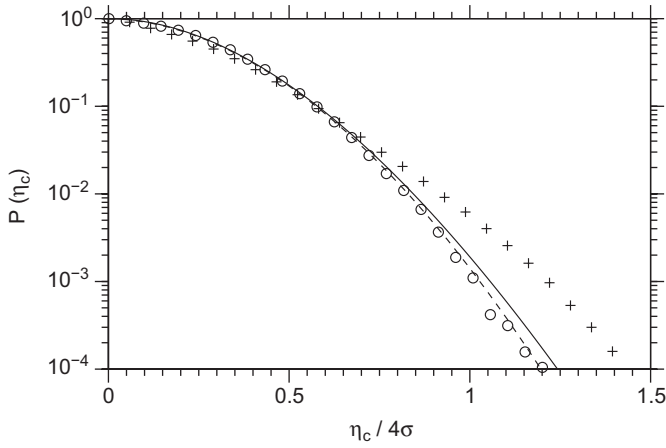


Fig. 9. Wave crest distribution for BFI = 1.0: Tayfun distribution (solid line); three-dimensional Forristall distribution (dashed line); simulations of long crested waves from the Euler equations (+); simulations of short crested waves from the Euler equations (o).

statistical properties of surface gravity waves (cf. Onorato et al., 2006). The limited, but significant, departure of the simulated wave crest distribution from the second-order wave crest distribution is most likely related to the effects of third and higher-order bound waves. As the degree of nonlinearity (BFI) is enhanced, however, this deviation increases, because the effect of the modulation instability becomes more relevant (see Onorato et al., 2006; Toffoli et al., 2008 for example).

When a broad-banded directional distribution is taken into account, the effect related to free modes is significantly reduced (see also Fig. 5). As a result, the deviation from the theoretical, second-order distributions vanishes. For low and moderate values of the BFI (i.e., 0.2 and 0.7), the Tayfun distribution (Eq. (5)) provides a satisfactory approximation of the simulated crest heights also at low probability levels ($P(\eta_c) = 0.0001$). This result is consistent with the findings presented by Socquet-Juglard et al. (2005), who performed numerical simulations of the surface elevation for a short crested wave field with $BFI \approx 0.7$ by using higher order nonlinear Schrödinger-type equations. If higher values of BFI (>0.7) are considered, however, the Tayfun distribution slightly overestimates our simulated crest heights.

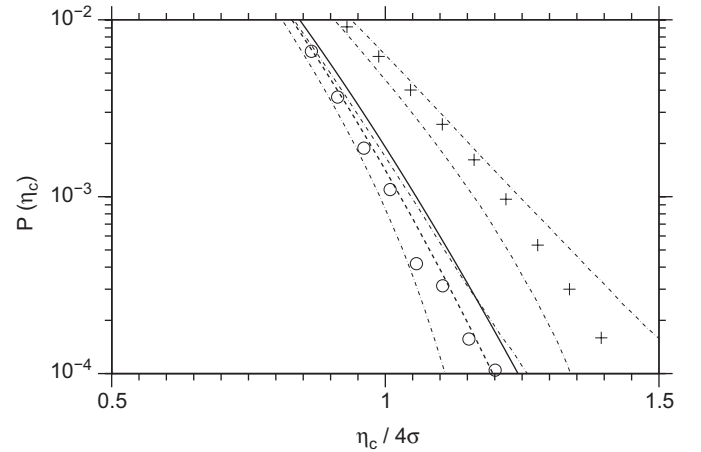


Fig. 10. Wave crest distribution and 95% confidence intervals for BFI = 1.0: Tayfun distribution (solid line); three-dimensional Forristall distribution (dashed line); simulations of long crested waves from the Euler equations (+); simulations of short crested waves from the Euler equations (o); 95% confidence intervals (dash-dotted line).

For probability levels greater than 0.0001, this departure appears to be statistically significant as the Tayfun distribution lays outside the 95% confidence intervals of the simulations (see Fig. 10). In this respect, it is interesting to note that the Tayfun distribution does not include directional effects explicitly as in the Forristall distribution. For short crested waves, the latter (Eq. (6)) indicates that directionality is responsible for a reduction of the crest height of about 2–4% than in the Tayfun distribution (see, e.g., Fig. 9); our simulations appear to be consistent with this (note that this finding does not invalidate the fact that the Tayfun distribution approximates field data well). Nonetheless, it appears clear that second-order effects dominate the statistical properties of the examined directional wave fields, while modulational instability effects become negligible. It should be mentioned, however, that the HOSM implemented for this research only accounts for a third order expansion of the vertical velocity. The addition of higher order terms, therefore, might slightly modify this result.

5. The wave trough distribution

In the case of deep water waves, it follows from Eq. (3) that an expression for the second-order wave trough can be written as

$$\eta_t = a_r - \frac{1}{2}k_p a_r^2. \quad (11)$$

By deriving the amplitude a_r from Eq. (11) and substituting it in the Rayleigh distribution, an expression for the exceedance probability can be written as follows (cf. Arhan and Plaisted, 1981):

$$P(\eta_t > \eta) = \exp \left[-\frac{8}{H_s^2 k_p^2} \left(\sqrt{1 - 2k_p \eta} - 1 \right)^2 \right]. \quad (12)$$

Likewise the Tayfun distribution, Eq. (12) is valid for long and short crested waves when a fixed location is considered (time series). However, according to the authors' knowledge, an analytical form for the second-order wave trough distribution including wave directional spreading explicitly (as, for example, in the Forristall distribution) has never been proposed. Therefore, in order to render explicit the effect of directionality on the statistical description of second-order wave troughs, series of random, time-domain profiles have been simulated using a second-order model (see, for example,

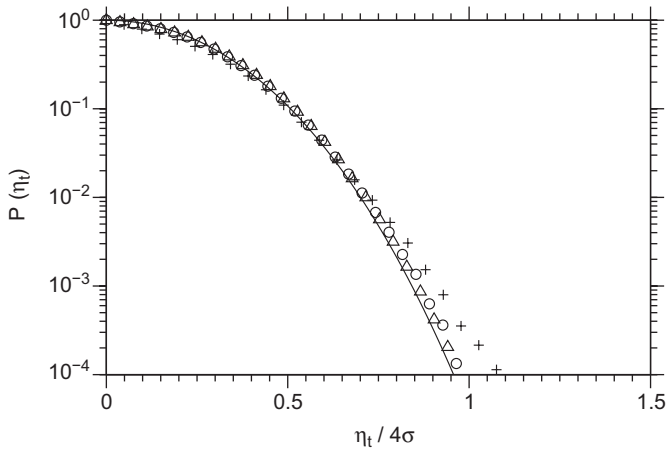


Fig. 11. Wave trough distribution for BFI = 0.2: theoretical (second-order) distribution (solid line); simulated, second-order short crested waves (Δ); simulations of long crested waves from the Euler equations (+); simulations of short crested waves from the Euler equations (o).

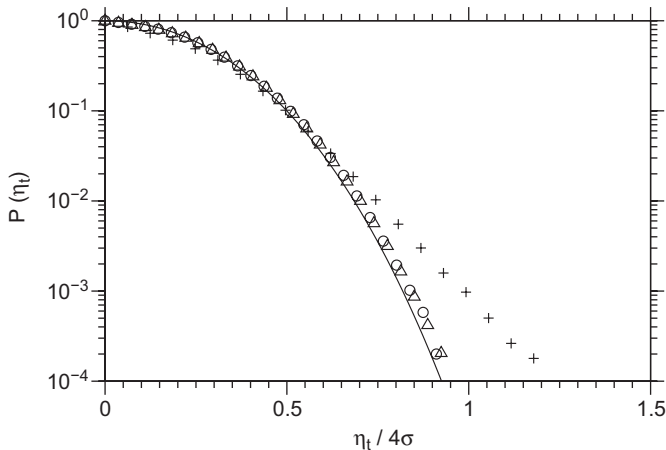


Fig. 12. Wave trough distribution for BFI = 0.7: theoretical (second-order) distribution (solid line); simulated, second-order short crested waves (Δ); simulations of long crested waves from the Euler equations (+); simulations of short crested waves from the Euler equations (o).

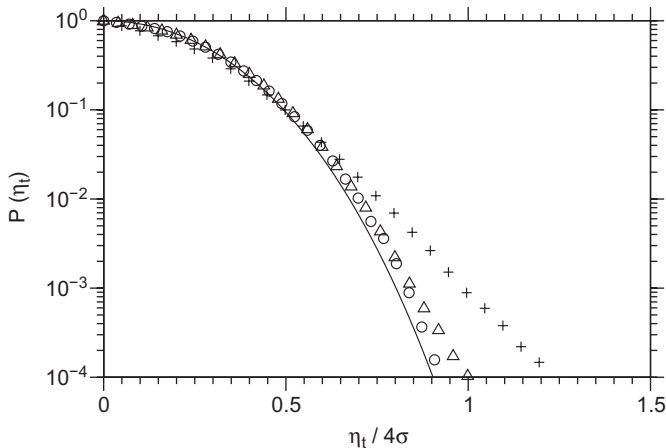


Fig. 13. Wave trough distribution for BFI = 1.0: theoretical (second-order) distribution (solid line); simulated, second-order short crested waves (Δ); simulations of long crested waves from the Euler equations (+); simulations of short crested waves from the Euler equations (o).

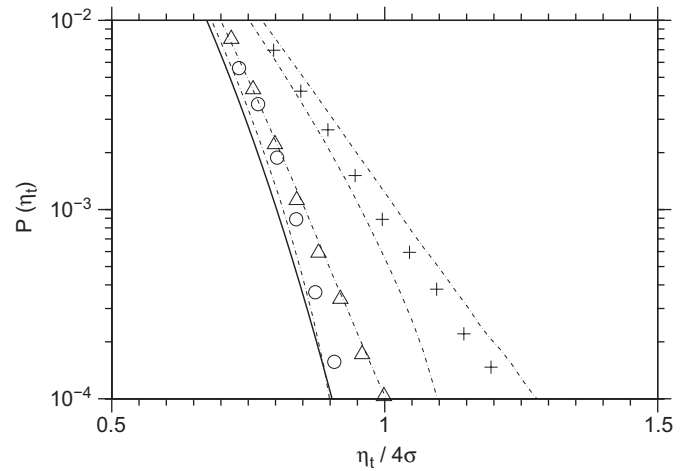


Fig. 14. Wave trough distribution and 95% confidence intervals for BFI = 1.0: theoretical (second-order) distribution (solid line); simulated, second-order short crested waves (Δ); simulations of long crested waves from the Euler equations (+); simulations of short crested waves from the Euler equations (o); 95% confidence intervals (dash-dotted line).

Sharma and Dean, 1981, for details). The spectral conditions used for the simulations of Eqs. (1) and (2) have been adopted to this end; details on the simulations of second-order waves can be found in Prevosto (1998). In Figs. 11–13, the wave trough distributions obtained from simulations of Eqs. (1) and (2) and second-order theory are presented.

In the case long crested waves are simulated, the effect of the modulational instability tends to enhance the depth of the wave troughs. This results in deviations from the second-order distribution given by Eq. (12) (see Toffoli et al., 2008, for details); this effect becomes more relevant if the BFI increases. As for the wave crests, this deviation is substantially reduced if the spectral energy is distributed on a broad range of directions. In this respect, simulations of short crested wave fields from Eqs. (1) and (2) show that the trough distribution deviates from the theoretical, second-order one (Eq. (12)), which slightly under predicts the simulated troughs (it lays outside the 95% confidence intervals as shown, for example, in Fig. 14). This is to some extent surprising since a similar distribution, Eq. (5), has proved to fit the simulated crests well. In this respect, second-order quasi-deterministic theory could provide a slightly better approximation (see Tayfun and Fedele, 2007b, for details). It is interesting to note, furthermore, that this departure does not increase in magnitude if BFI is increased.

Despite the under prediction of Eq. (12), however, the simulations of second-order, short crested waves strongly indicate that second-order theory provides a good approximation of the trough distribution obtained from Eqs. (1) and (2). In this respect, it seems that the second-order effect on the wave troughs is more sensitive to the directional spreading than the one on the wave crests, as a significant enhancement of the trough depth is already observed for low degrees of nonlinearity. For higher values of the BFI (>0.7), however, the amplitude of the wave troughs predicted by the simulations of second-order, short crested waves slightly deviates from the results of Eqs. (1) and (2) at low probability levels (0.0001). Nonetheless, this departure does not appear to be statistically significant (see Fig. 14).

6. Conclusions

It is clearly established that, for deep water waves, the modulational instability may produce a significant departure

from Gaussian statistics as it enhances the probability of occurrence for extreme waves. When directional wave components are considered, however, this deviation is reduced. In order to analyze the statistical properties of directional wave fields, numerical simulations of the Euler equations have been used. To this end, the higher order spectral method (HOSM) proposed by West et al. (1987) is applied for the numerical solution of the Euler equations. A set of numerical experiments have been performed using a broad-banded directional wave field (wind sea) in water of infinite depth to investigate whether the modulational instability may produce a significant deviation from second-order statistical distributions of wave crests and troughs.

As a general result, our simulations have shown that the coexistence of different directional components reduces the skewness and kurtosis of the surface elevation. The latter, in particular, does not significantly depart from the value expected for Gaussian, linear processes. In other words, the occurrence of extreme events in broad-banded directional wave fields of infinite water depth seems to be neither more frequent nor higher than the second-order wave theory predicts.

The reduction of the value of the statistical moments leads to a significant modification of the tail of wave crest distribution.

In the present study, the probability distribution of wave crests has been compared with the second-order, theory-based Tayfun (1980) and Forristall (2000) distributions. Whereas the first is derived under the assumption of a narrow-banded wave spectrum, the latter includes wave directional spreading explicitly. For low and moderated degrees of nonlinearity ($BFI = 0.2$ and 0.7), the directional spreading does not produce any significant effect on the tail of the second-order wave crest distribution; both distributions give very close predictions. Moreover, considering that the coexistence of directional wave components reduces the modulational instability, the crest heights simulated with the Euler equations are fitted by second-order based distributions well. These findings are consistent with the results presented by Socquet-Juglard et al. (2005). For higher degrees of nonlinearity ($BFI > 0.7$), however, the directional spreading slightly changes the tail of the second-order wave crest distribution in agreement with the Forristall distribution. Therefore, it may be concluded that modulation instability does not have a significant influence on the wave crest distribution, when the spectral energy is distributed on a broad range of directional components.

For long crested wave fields, not only does modulational instability have effects on the crest heights, but also on the wave troughs. In particular, we have observed that wave troughs can be significantly deeper than second-order theory would predict. The directional spreading, however, tends to cancel these effects. Unlike for the wave crest, the wave trough distribution slightly deviates from the theoretical, second-order distribution, also at low degrees of nonlinearity; simulated troughs tend, in fact, to remain deeper. Due to the lack of theoretical distribution for the wave troughs in short crested conditions, an additional set of short crested second-order wave profiles have been simulated with similar spectral conditions which were used for the simulation of the Euler equations. The comparison of second-order simulated profiles and numerical simulations of the Euler equations indicates that the modulational instability does not have any significant influence on the wave trough statistics if a broad-banded directional spectrum is accounted for. The observed under-estimation of the theoretical distribution is therefore likely due to directional spreading effects on the second-order interaction.

The results presented in the paper are valid within the framework of the adopted numerical approach which is based on the third order expansion of the vertical velocity and hence it is not a fully nonlinear solution. Further, it does not account for

wave breaking. These limitations might affect the statistics presented. Furthermore, the results presented are developed for an unimodal spectral distribution with a broad-banded energy spread, thus more narrow-banded directional spectra as well as bimodal wave fields are not considered. On the whole, however, it can be concluded that second-order theory provides a satisfactory approximation of the statistical properties of broad-banded directional wave fields simulated with HOSM. However, a comparison of the numerical results with field data as well as a more comprehensive investigation of the effects related to different directional bandwidths and spectral bimodality is called for before a firm conclusion can be reached about the applicability of the second-order theory for extreme wave prediction.

Acknowledgments

This work was carried out in the framework of the E.U. project SEAMOCS (contract MRTN-CT-2005-019374). We are thankful to Jason McConochie of Woodside Energy Ltd, Western Australia for his comments on industrial applications of the wave trough probability distributions. The E.U. project SAFE OFFLOAD (contract TST4-CT-2005-012560) is also acknowledged.

References

- Annenkov, S.Y., Shrira, V.I., 2001. Numerical modeling of water-wave evolution based on the Zakharov equation. *Journal of Fluid Mechanics* 449, 341–371.
- Arhan, M., Plaisted, R.O., 1981. Non-linear deformation of sea-wave profiles in intermediate and shallow water. *Oceanologica Acta* 4 (2), 107–115.
- Bitner-Gregersen, E., Hagen, Ø., 2003. Effects of two-peak spectra on wave crest statistics. In: *Proceedings of the 22nd International Conference on Offshore Mechanics and Arctic Engineering (OMAE)*. Cancun, Mexico, June 8–13.
- Bitner-Gregersen, E., Magnusson, A.K., 2004. Extreme events in field data and in a second order wave model. In: *Proceedings of the Rogue Waves 2004*. Brest, France, October 20–31.
- Clamond, D., Grue, J., 2001. A fast method for fully nonlinear water-wave computations. *Journal of Fluid Mechanics* 447, 337–355.
- Clamond, D., Francius, M., Grue, J., Kharif, C., 2006. Long time interaction of envelope solitons and freak wave formations. *European Journal of Mechanics B/Fluids* 25, 536–553.
- Dommermuth, D.G., Yue, D.K., 1987. A high-order spectral method for the study of nonlinear gravity waves. *Journal of Fluid Mechanics* 184, 267–288.
- Dysthe, K.B., 1979. Note on the modification of the nonlinear Schrödinger equation for application to deep water waves. *Proceedings of the Royal Society of London A* 369, 105–114.
- Ewans, K.C., 1998. Observations of directional spectrum of fetch-limited waves. *Journal of Physical Oceanography* 28, 495–512.
- Fedele, F., Arena, F., 2005. Weakly nonlinear statistics of high random waves. *Physics of Fluids* 17 (1), 1–10.
- Forristall, G., 2000. Wave crests distributions: observations and second-order theory. *Journal of Physical Oceanography* 30, 1931–1943.
- Gibson, R.S., Swan, C., Tromans, P.S., 2007. Fully nonlinear statistics of wave crest elevation calculated using a spectral response surface method: application to unidirectional sea states. *Journal of Physical Oceanography* 37, 3–15.
- Gramstad, O., Trulsen, K., 2007. Influence of crest and group length on the occurrence of freak waves. *Journal of Fluid Mechanics* 582, 463–472.
- Hasselmann, K., 1962. On the non-linear energy transfer in a gravity-wave spectrum. Part 1: general theory. *Journal of Fluid Mechanics* 12, 481–500.
- Janssen, P.A.E.M., 2003. Nonlinear four-wave interaction and freak waves. *Journal of Physical Oceanography* 33 (4), 863–884.
- Komen, G., Cavaleri, L., Donelan, M., Hasselmann, K., Hasselmann, H., Janssen, P., 1994. *Dynamics and Modeling of Ocean Waves*. Cambridge University Press, Cambridge.
- Longuet-Higgins, M., 1963. The effect of non-linearities on statistical distribution in the theory of sea waves. *Journal of Fluid Mechanics* 17, 459–480.
- Mitsuyasu, H., Tsubota, F., Suhara, T., Mizuno, S., Ohkusu, M., Honda, T., Rikiishi, K., 1975. Observations of the directional spectrum of ocean waves using a cloverleaf buoy. *Journal of Physical Oceanography* 5, 750–760.
- Mori, N., Janssen, P.A.E.M., 2006. On kurtosis and occurrence probability of freak waves. *Journal of Physical Oceanography* 36, 1471–1483.
- Mori, N., Yasuda, T., 2002. Effects of high-order nonlinear interactions on unidirectional wave trains. *Ocean Engineering* 29, 1233–1245.
- Onorato, M., Osborne, A., Serio, M., Bertone, S., 2001. Freak wave in random oceanic sea states. *Physical Review Letters* 86 (25), 5831–5834.
- Onorato, M., Osborne, A.R., Serio, M., 2002a. Extreme wave events in directional random oceanic sea states. *Physics of Fluids* 14 (4), 25–28.

- Onorato, M., Osborne, A.R., Serio, M., Resio, D., Puskarev, A., Zakharov, V.E., Brandini, C., 2002b. Freely decaying weak turbulence for sea surface gravity waves. *Physical Review Letters* 89 (4.144501).
- Onorato, M., Osborne, A., Serio, M., Cavaleri, L., Brandini, C., Stansberg, C., 2006. Extreme waves, modulational instability and second order theory: wave flume experiments on irregular waves. *European Journal of Mechanics B/Fluids* 25, 586–601.
- Petrova, P., Cherneva, Z., Guedes Soares, C., 2006. Distribution of crest heights in sea states with abnormal waves. *Applied Ocean Research* 28, 235–245.
- Prevosto, M., 1998. Effect of directional spreading and spectral bandwidth on the nonlinearity of the irregular waves. In: *Proceedings of the 8th International Offshore and Polar Engineering (ISOPE) Conference*, Montréal, Canada, May 24–29.
- Prevosto, M., Krogstad, H., Robin, A., 2000. Probability distributions for maximum wave and crest heights. *Coastal Engineering* 40, 329–360.
- Sharma, N., Dean, R., 1981. Second-order directional seas and associated wave forces. *Society of Petroleum Engineering Journal* 4, 129–140.
- Socquet-Juglard, H., Dysthe, K., Trulsen, K., Krogstad, H., Liu, J., 2005. Distribution of surface gravity waves during spectral changes. *Journal of Fluid Mechanics* 542, 195–216.
- Tanaka, M., 2001a. A method of studying nonlinear random field of surface gravity waves by direct numerical simulations. *Fluid Dynamics Research* 28, 41–60.
- Tanaka, M., 2001b. Verification of Hasselmann's energy transfer among surface gravity waves by direct numerical simulations of primitive equations. *Journal of Fluid Mechanics* 444, 199–221.
- Tanaka, M., 2007. On the role of resonant interactions in the short-term evolution of deep-water ocean spectra. *Journal of Physical Oceanography* 37, 1022–1036.
- Tayfun, M.A., 1980. Narrow-band nonlinear sea waves. *Journal of Geophysical Research* 85 (C3), 1548–1552.
- Tayfun, M.A., 2006. Statistics of nonlinear wave crests and groups. *Ocean Engineering* 33, 1589–1622.
- Tayfun, M.A., Fedele, F., 2006. Wave-height distributions and nonlinear wave effects. In: *Proceedings of the 25th International Conference on Offshore Mechanics and Arctic Engineering (OMAE)*. Hamburg, Germany, June 4–9.
- Tayfun, M.A., Fedele, F., 2007a. Expected shape of extreme waves in storm seas. In: *Proceedings of the 26th International Conference on Offshore Mechanics and Arctic Engineering (OMAE)*. San Diego, CA, USA, June 10–15.
- Tayfun, M.A., Fedele, F., 2007b. Wave-height distributions and nonlinear effects. *Ocean Engineering* 34, 1631–1649.
- Toffoli, A., Lefèvre, J., Bitner-Gregersen, E., Monbaliu, J., 2005. Towards the identification of warning criteria: analysis of a ship accident database. *Applied Ocean Research* 27, 281–291.
- Toffoli, A., Onorato, M., Monbaliu, J., 2006. Wave statistics in unimodal and bimodal seas from a second-order model. *European Journal of Mechanics B/Fluids* 25, 649–661.
- Toffoli, A., Onorato, M., Bitner-Gregersen, E., Osborne, A.R., Babanin, A.V., 2008. Surface gravity waves from direct numerical simulations of the Euler equations: a comparison with second-order theory. *Ocean Engineering* 35 (3–4), 367–379.
- Tsai, W.-T., Yue, D.K., 1996. Computation of nonlinear free-surface flows. *Annual Reviews in Fluid Mechanics* 28, 249–278.
- Waseda, T., 2006. Impact of directionality on the extreme wave occurrence in a discrete random wave system. In: *Proceedings of the 9th International Workshop on Wave Hindcasting and Forecasting*. Victoria, Canada, September 24–29.
- West, B.J., Brueckner, K.A., Jand, R.S., Milder, D.M., Milton, R.L., 1987. A new method for surface hydrodynamics. *Journal of Geophysical Research* 92 (C11), 11803–11824.
- Whitham, G., 1974. *Linear and Nonlinear Waves*. Wiley Interscience, New York.
- Zakharov, V., 1968. Stability of period waves of finite amplitude on surface of a deep fluid. *Journal of Applied Mechanics and Technical Physics* 9, 190–194.
- Zakharov, V.E., Dyachenko, A.I., Vasilyev, O.A., 2002. New method for numerical simulation of a nonstationary potential flow of incompressible fluid with a free surface. *European Journal of Mechanics B/Fluids* 21, 283–291.